PERGAMON

International Journal of Heat and Mass Transfer 44 (2001) 551–574

International Journal of HEAT and MASS TRANSFER

www.elsevier.com/locate/ijhmt

Enhancement of heat transfer by a combination of three-start spirally corrugated tubes with a twisted tape

Ventsislav Zimparov*

Gabrovo Technical University, 4 Hadji Dimitar Street, BG-5300 Gabrovo, Bulgaria

Received 17 March 2000

Abstract

Heat transfer and isothermal friction pressure drop results have been obtained experimentally for two three-start spirally corrugated tubes combined with five twisted tape inserts with different relative pitches in the range of Reynolds number 3×10^3–6×10^4. The characteristic parameters of the tubes are: height to diameter ratio, $e/D_i = 0.0407$ and 0.0569; and relative pitch, $H/D_i = 15.3$, 12.2, 7.7, 5.8, 4.7. Significantly, higher friction factor and inside heat-transfer coefficients than those of the smooth tube under the same operating conditions have been observed. Extended performance evaluation criteria (PEC) equations for enhanced heat transfer surfaces have been used to assess the multiplicative effect. Thermodynamic optimum can be defined by minimizing the entropy generation number compared with the relative increase of heat transfer rate or relative reduction of heat transfer area. © 2001 Elsevier Science Ltd. All rights reserved.

Keywords: Enhancement of heat transfer; Spirally corrugated tube; Twist tape insert; Performance evaluation; Entropy generation minimization

1. Introduction

The performance of a conventional heat exchanger, which is an essential unit in heat extraction and recovery systems, can be substantially improved by a number of augmentation techniques. Common thermal–hydraulic goals are to reduce the size of heat exchanger required for specified heat duty, to upgrade the capacity of an existing heat exchanger, to reduce the approach temperature difference for the process streams, or to reduce the pumping power [1]. A preferred approach to the problem of increasing heat exchanger effectiveness, while maintaining minimum heat exchanger size and operational cost, is to increase the heat transfer exchange rate.

Many different methods have been considered to increase the rate of heat transfer in forced convection while reducing the size of the heat exchanger and effecting energy savings [1–3]. Surface methods include any techniques, which directly involve the heat exchanger surface. They are used on the side of the surface that comes into contact with a fluid of low heat transfer coefficient in order to reduce the thickness of the boundary layer and to introduce better fluid mixing. The primary mechanisms for thinning the boundary layer are increased stream velocity and turbulent mixing. Secondary recirculation flows can further enhance convective transfer. Flows from the core to the wall reduce the thickness of the boundary layer and the secondary flows

* Fax: +359-66-24856.
E-mail address: vdzim@tugab.bg (V. Zimparov).

0017-9310/01/$ - see front matter © 2001 Elsevier Science Ltd. All rights reserved.
PII: S0017-9310(00)00126-5

Nomenclature

A	heat transfer surface area (m^2)
D	tube diameter (m)
e	ridge height (m)
k	thermal conductivity (W m^{-1} K^{-1})
L	tube length (m)
$\dot{m}$	mass flow rate in the tube (kg s^{-1})
N_t	number of tubes
P	pumping power (W)
p	pitch of ridging (m)
Δp	pressure drop (Pa)
$\dot{Q}$	heat transfer rate (W)
$\dot{S}_{gen}$	rate of entropy generation (W K^{-1})
T	temperature (K)
ΔT	temperature difference (K)
u	flow velocity (m s^{-1})
U	overall heat transfer coefficient (W m^{-2} K^{-1})
W	mass flow rate in the heat exchanger (kg s^{-1})

Greek symbols

α	heat transfer coefficient (W m^{-2} K^{-1})
β	helix angle of rib (°)
ϑ	temperature difference between the wall and the fluid, $T_w - T$ (K)
μ	dynamic viscosity (Pa s)
ρ	fluid density (kg m^{-3})

Dimensionless groups

A_*	dimensionless heat transfer surface (A_R/A_S)
D_*	dimensionless tube diameter (D_R/D_S)
L_*	dimensionless tube length (L_R/L_S)
f	fanning friction factor ($2\tau_w/\rho u_m^2$)
Nu	Nusselt number ($\alpha_i D/k_f$)
N_S	augmentation entropy generation number
N_*	ratio of the number of tubes ($N_{t,R}/N_{t,S}$)
Pr	Prandtl number ($\mu c_p/k_f$)
P_*	dimensionless pumping power (P_R/P_S)
Q_*	dimensionless heat transfer rate ($\dot{Q}_R/\dot{Q}_S$)
Re	Reynolds number ($\rho u_m D/\mu$)
St	Stanton number ($\alpha_i/\rho u_m c_p$)
ΔT_i^*	dimensionless inlet temperature difference between the hot and the cold streams ($\Delta T_{i,R}^+/\Delta T_{i,S}^+$)
$u_{m,*}$	dimensionless flow velocity ($u_{m,R}/u_{m,S}$)
W_*	dimensionless mass flow rate (W_R/W_S)
β_*	$\beta/90$
ε_*	ratio of heat exchanger effectiveness ($\varepsilon_R/\varepsilon_S$)
ϕ_o	irreversibility distribution ratio

Subscripts

f	fluid
i	inside
i	value at $x = 0$
m	mean value
R	rough tube
S	smooth tube
o	outside
o	value at $x = L$
w	wall

from the wall to the core promote mixing. Flow separation and reattachment within the flow channel also contribute to heat transfer enhancement.

Some of the existing methods for enhancing heat transfer in a single-phase, fully developed turbulent flow in a round tube are of one of the two types, (a) methods in which the inner surface of the tube is roughened, e.g. with repeated or helical ribbing, by sanding, or with internal fins; and (b) methods in which a heat transfer promoter, e.g. a twisted tape, disk or streamlined shape, is inserted into the tube.

It is well known that two or more of the existing techniques can be utilized simultaneously to produce an enhancement larger than that produced by only one technique. The combination of different techniques acting simultaneously is known as compound augmentation. This is an emerging area of interest and holds promise for practical applications. Interactions between different augmentation methods contribute to greater values of the heat transfer coefficients compared to the sum of the corresponding values for the individual techniques used alone. Preliminary studies in compound passive augmentation techniques are encouraging. Some examples are: rough tube wall with twisted tape inserts [4] and grooved rough tube with twisted tape [5].

Many previous surveys indicate that the corrugated tubes are among the most effective and practical methods for augmenting single-phase heat transfer in tubes. It is reasonable to assume that a combination of a corrugated tube with twisted tape would be superior to either combination of passive surface techniques.

This study reports on an experimental investigation to see whether or not heat transfer can be enhanced by the multiplicative effect of a corrugated tube combined with a twisted tape.

2. Experimental program

In the present experimental program two three-

start spirally corrugated tubes of varying geometries combined with five twisted tapes with different pitches have been studied. The smooth tube had an inside diameter of 16.0 mm with wall thickness of 1.0 mm before rolling operation. A smooth tube was used for standardizing the experimental set-up and for comparing the enhancement in heat transfer and fluid friction. The enhanced tubes were manufactured from smooth tubes with a fabrication technique, which embosses an internal projection, also known as a ridge, in registration with an external groove. The characteristic parameters — pitch of corrugation p, height of corrugation e, spiral angle β and dimensionless parameters e/D_i, p/e, β_*, are listed in Table 1. The twisted tape comprising heat-treated brass tape has a thickness of 0.8 mm and a width of 12.5 mm. With the length of the tape in 360° twist defined as H, five different tapes were used: $H/D_i = 15.3$, 12.2, 7.7, 5.8 and 4.7.

Full details of the experimental set-up consisting of two heat transfer tubes, 1200-mm long, in a conventional recirculating system can be found in [6]. The pressure difference across the heat transfer section was measured and friction coefficients were calculated. The heating section was heated by condensing steam generated into a boiler. The flow rate of the test fluid, the tube wall temperatures, the inlet and outlet water temperatures and the temperature of the saturated steam were measured. The water flow rate was measured with a calibrated orifice meter and the accuracy of the measurement was estimated to be 2% while that of the pressure-drop measurement was 5%. The inlet and outlet temperatures of the cooling water was measured by calibrated 0.1°C accurate mercury-in-glass thermometers. The wall temperatures were measured by 12 copper-constantan thermocouples with the same accuracy. The bulk temperature of the water ranged from 48 to 92°C and the corresponding variation of the Prandtl number was 3.7–1.9. The heat transfer coefficient was calculated from the heat flux density at the wall as measured in the heat balance.

3. Results and discussion

The isothermal pressure drop studies were conducted at different temperatures of the water in the range from 45 to 90°C in all the tubes over a range of Reynolds number $4 \times 10^3 < Re < 6 \times 10^4$. The friction coefficients for the smooth tube were satisfactorily correlated by the Blasius equation

$$f = 0.079 Re^{-0.25}, \tag{1}$$

over a range of Reynolds number $4 \times 10^3 < Re < 6 \times 10^4$ with a standard deviation of $\pm 3\%$ and this equation was used for calibration of the experimental set-up.

As expected, the turbulent flow friction coefficient f was significantly higher than that in the smooth tube f_S under the same operating conditions Figs. 1 and 2. A characteristic feature of the flow is that even at high flow rates, the friction factor continues to decrease with the increase of Re although not so rapidly as in the smooth tube. The isothermal friction coefficients for straight flow and swirl flow in the corrugated tubes increase when the relative pitch H/D_i decreases. The friction factor data were correlated by the following equation:

$$f = c_f Re^m, \tag{2}$$

obtained by a curve-fitting procedure. The values of c_f and m were determined for each tube and are listed in Table 2.

Heat transfer studies in multi-start spirally corrugated tubes were carried out to obtain values for the

Table 1
Characteristic parameters of the tubes

Number	D_o (mm)	D_i (mm)	e (mm)	p (mm)	β (°)	e/D_i	p/e	β_*	H/D_i
4040	15.72	13.68	0.557	5.97	67.4	0.0407	10.73	0.749	–
4041	15.72	13.68	0.557	5.97	67.4	0.0407	10.73	0.749	15.4
4042	15.72	13.68	0.557	5.97	67.4	0.0407	10.73	0.749	12.3
4043	15.72	13.68	0.557	5.97	67.4	0.0407	10.73	0.749	7.8
4044	15.72	13.68	0.557	5.97	67.4	0.0407	10.73	0.749	5.9
4045	15.72	13.68	0.557	5.97	67.4	0.0407	10.73	0.749	4.8
4030	15.72	13.73	0.781	5.82	68.0	0.0569	7.45	0.755	–
4031	15.72	13.73	0.781	5.82	68.0	0.0569	7.45	0.755	15.3
4032	15.72	13.73	0.781	5.82	68.0	0.0569	7.45	0.755	12.2
4033	15.72	13.73	0.781	5.82	68.0	0.0569	7.45	0.755	7.7
4034	15.72	13.73	0.781	5.82	68.0	0.0569	7.45	0.755	5.8
4035	15.72	13.73	0.781	5.82	68.0	0.0569	7.45	0.755	4.7

water side heat transfer coefficients h_i and the steam condensing coefficients h_o. Since the metal wall temperatures were measured, the individual film coefficients were determined. The smooth tube heat transfer coefficients were found to agree with ±10% of the Gnielinski correlation [7]

$$Nu = 0.012(Re^{0.87} - 280)Pr^{0.4}, \quad (3)$$

in the range $1.5 \leq Pr \leq 500$, $3 \times 10^3 \leq Re \leq 10^6$. Figs. 3 and 4 show the heat transfer data in the form $Nu_i Pr^{-0.4}$ as a function of the Reynolds number Re, a counterpart of the friction factor data shown on

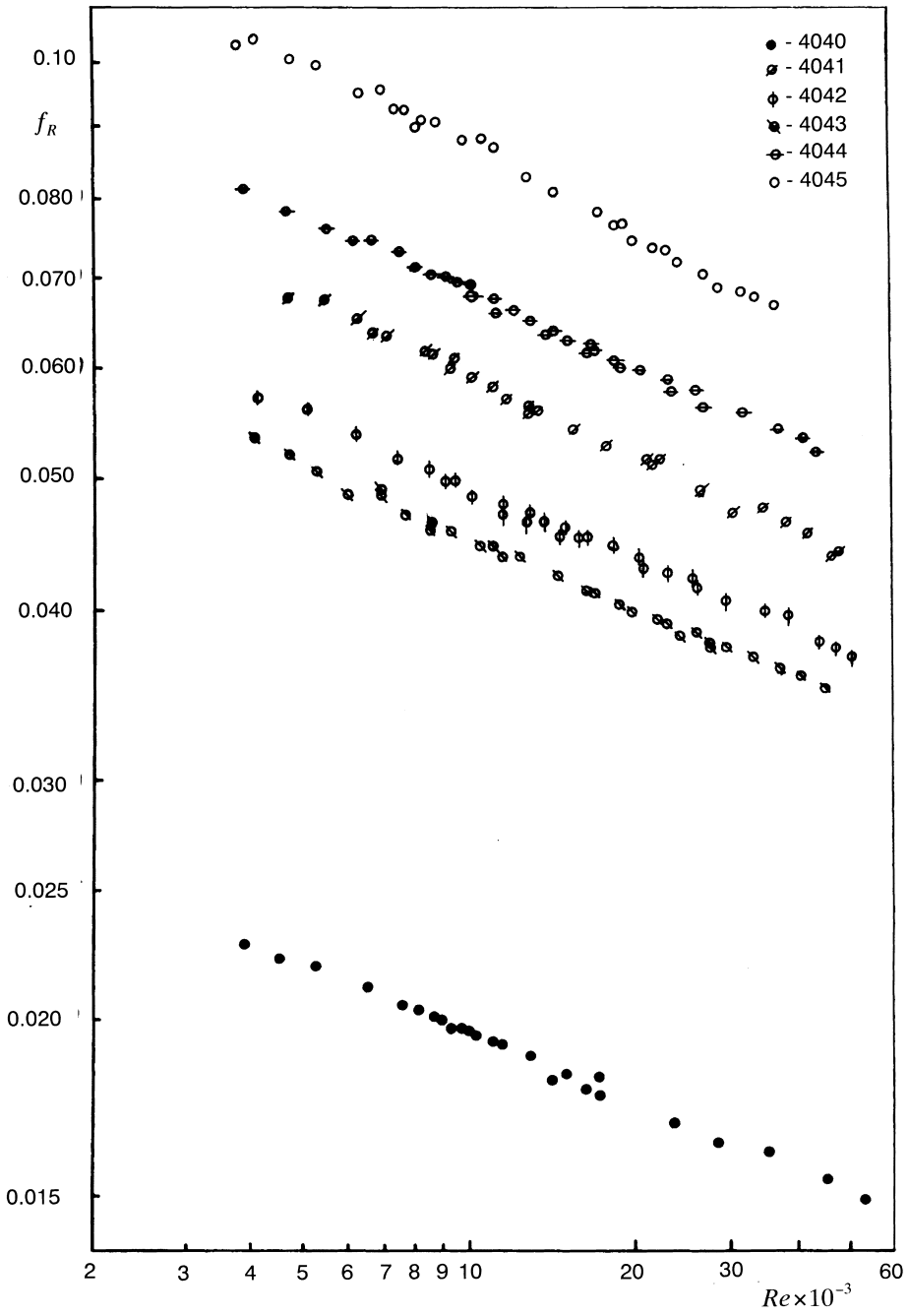

Fig. 1. Variation of friction factor vs. Reynolds number.

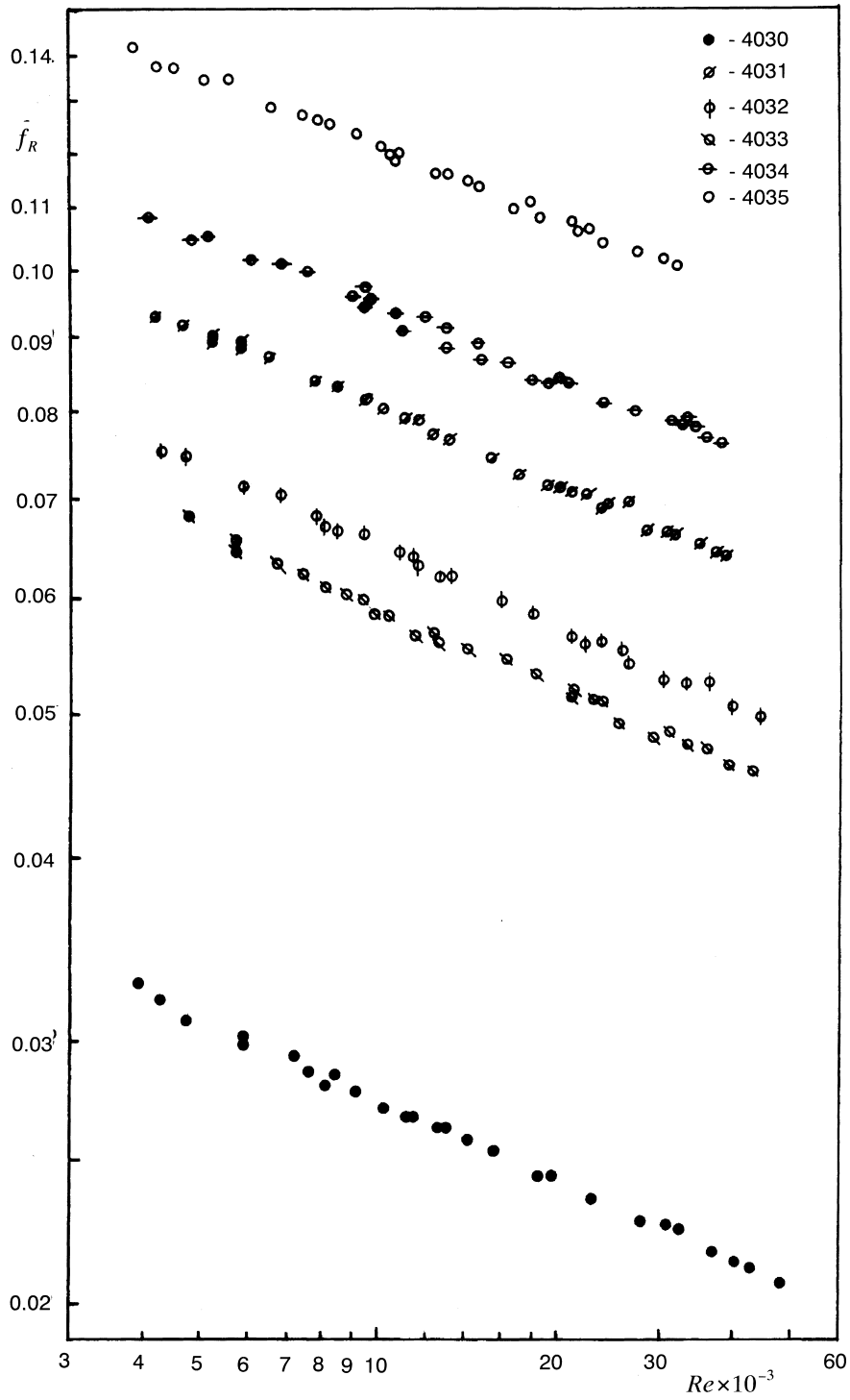

Fig. 2. Variation of friction factor vs. Reynolds number.

Table 2
Values of the friction coefficients

Number	c_f	m
4040	0.117	−0.192
4041	0.229	−0.176
4042	0.260	−0.181
4043	0.378	−0.202
4044	0.383	−0.187
4045	0.409	−0.170
4030	0.148	−0.182
4031	0.297	−0.175
4032	0.335	−0.178
4033	0.390	−0.171
4034	0.432	−0.165
4035	0.526	−0.160

Table 3
Values of the heat transfer coefficients

Number	c_h	n	Re	c_h	n	Re
4040	0.0167	0.897				
4041	0.0187	0.900				
4042	0.0244	0.882				
4043	0.0028	1.130	< 26 400	0.549	0.612	> 26 400
4044	0.0048	1.108	< 20 500	0.521	0.635	> 20 500
4045	0.0019	1.223	< 21 100	1.535	0.548	> 21 100
4030	0.0390	0.823				
4031	0.0213	0.918	< 30 150	0.437	0.625	> 30 150
4032	0.0143	0.970	< 30 550	0.710	0.592	> 30 550
4033	0.0057	1.096	< 23 800	0.294	0.704	> 23 800
4034	0.0020	1.239	< 21 200	0.545	0.677	> 21 200
4035	0.0009	1.344	< 23 400	3.536	0.521	> 23 400

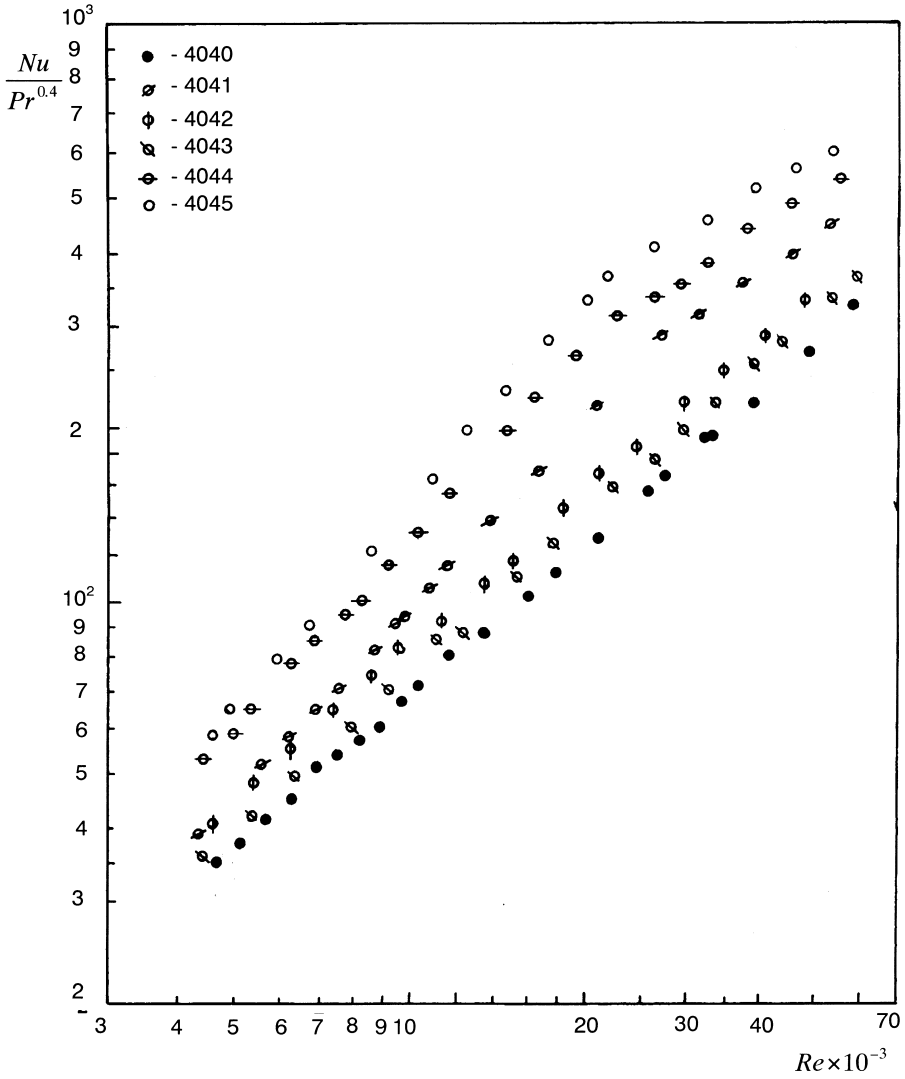

Fig. 3. Water-side heat transfer coefficient vs. Reynolds number.

Figs. 1 and 2. We can also see that the water-side heat transfer coefficients are particularly high when the height to diameter ratio e/D_i increases and the relative pitch H/D_i decreases. In the course of the heat transfer experiments an unexpected behavior of the ratio $Nu_R/Nu_S = f(Re)$ emerged for $Re \sim 2.5 \times 10^4$ when the relative pitch began to diminish. For the tubes 4043–4045 and 4031–4035 the ratio $Nu_R/Nu_S = f(Re)$ approaches maximum at $Re \sim 2.5 \times 10^4$ and then decreases gradually. This kind of behavior has not been observed for the rest of the tubes. Therefore, the heat transfer data were correlated with two different curves in the form

$$Nu_i Pr^{-0.4} = c_h Re^n, \tag{4}$$

by a curve fitting procedure and the values of the constants c_h and n, for each tube, are listed in Table 3. The values for Nu_R/Nu_S in the range of Re studied are showed in Table 4.

4. Performance evaluation

As preliminary design guidance to the selection of a technique, the heat transfer efficiency can be evaluated based on the power consumption per unit mass of the fluid. The criterion i_E [5] is defined as the ratio between the heat transfer coefficient for the tube using the heat transfer promoter and the value for a smooth tube at

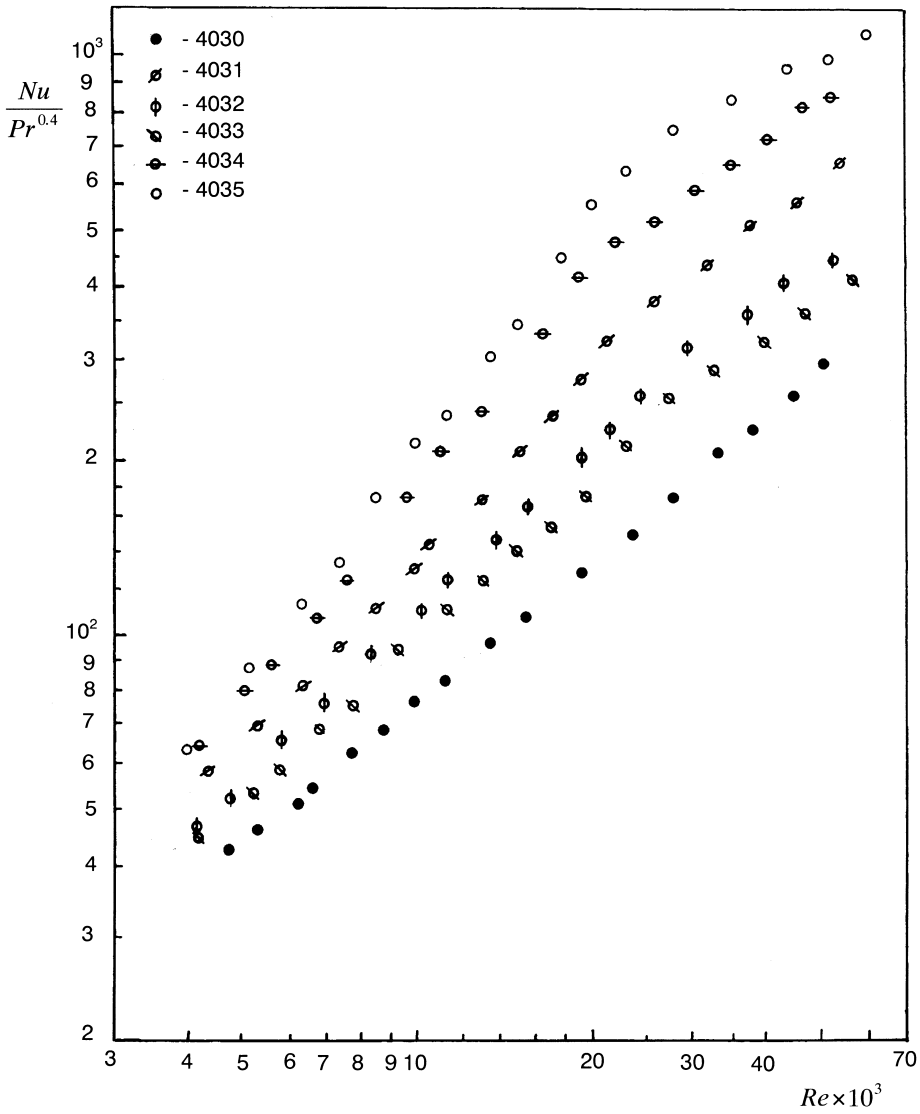

Fig. 4. Water-side heat transfer coefficient vs. Reynolds number.

the same level of power. Following [5] the criterion i_E can be defined as

$$i_E = \frac{Nu_R/Nu_S}{(f_R/f_S)^{0.291}} = f(Re_S). \quad (5)$$

With the twisted tape alone, i_E was in the general flow, in value of the order of 1.0–1.2. When an internally grooved or corrugated tube was alone used, $i_E = 1.5$–2.0 for $Re > 10^4$. When a counterclockwise twisted tape was used in conjunction with an internally grooved tube [5], i_E attained values of 2.5–3.3. Fig. 5 represents the values of i_E for all the combinations of a corrugated tube and a twisted tape insert investigated together with those obtained in the previous studies [4,5]. With an appropriate selection of the geometric parameters, e/D_i and H/D_i, a very great improvement in the heat transfer efficiency (i_E) = 2.7–4.2 could be reached.

On the basis of the first law analysis, several authors [8–12] have proposed performance evaluation criteria (PEC) which define the performance benefits of an exchanger having enhanced surfaces, relative to a standard exchanger with smooth surfaces subject to various design constraints. On the other hand, it is well established that the minimization of the entropy generation in any process leads to the conservation of useful energy. A solid thermodynamic basis to evaluate the merit of augmentation techniques by second law analysis has been proposed by Bejan [13,14] and developed the entropy generation minimization (EGM) method also known as 'thermodynamic optimization'. The ultimate purpose is to evaluate the advantage of a given augmentation technique by comparing the rates of entropy generation in an augmented duct and in a reference smooth one.

The method of Bejan [13,14] does not include the effect of the variation in fluid temperature similar to that presented in tubular heat exchangers. Extended PEC equations including the fluid temperature variation along the heat transfer passage for heat transfer from ducts with constant wall temperature have been developed by Zimparov [15]. These PEC equations have been used to assess the multiplicative effect of a corrugated tube combined with a twisted tape. The equations originate from various design constraints and generalize the PEC for enhanced heat transfer techniques obtained by means of the first law analysis. The application of this more comprehensive treatment of PEC compared to previous references is illustrated by the analysis of the heat transfer and fluid friction characteristics of the multi-start spirally corrugated tubes combined with five twisted tapes having different pitches.

When an enhanced tube is being considered for the replacement of a smooth one, there are many possible effects on the performance. The design constraints imposed on the exchanger flow rate and velocity cause key differences among the possible PEC relations on the basis of the first law analysis [11,12]. The increased friction factor due to augmented surfaces may require a reduced velocity to satisfy a fixed pumping power (or pressure drop) constraint. However, if the mass flow rate is reduced, it is possible to maintain a constant flow frontal area at reduced velocity. In many cases the heat exchanger flow rate is specified and a flow rate reduction is not permitted. Despite of the fact that a large number of possible PEC can be defined [16], the PEC as suggested by Webb and Bergles [11,12] characterize almost all the PEC and some of them are shown below. The equations are developed for tubes of different diameters and heat transfer and friction factors based on the presentation format of performance data for enhanced tubes [17]. The relative equations for single-phase flow inside enhanced tubes are:

$$A_* = N_* L_* D_*, \quad (6)$$

$$P_* = W_* \Delta p_* = \frac{f_R}{f_S D_* L_* N_* u_{m,*}^3} = \frac{W_*^3 L_*}{N_*^2 D_*^5} \frac{f_R}{f_S}, \quad (7)$$

$$Q_* = W_* \varepsilon_* \Delta T_i^*, \quad (8)$$

$$W_* = u_{m,*} D_*^2 N_* = \frac{Re_R}{Re_s} D_* N_*, \quad (9)$$

$$\Delta p_* = \left(\frac{f_R}{f_S}\right) \frac{L_*}{D_*} u_{m,*}^2 = \left(\frac{f_R}{f_S}\right) \frac{L_*}{D_*^3} \frac{Re_R^2}{Re_S^2} \quad (10)$$

Following Bejan [13,14] the thermodynamic impact of the augmentation technique is defined by the aug-

Table 4
Increase of the heat transfer coefficient

Number	Nu_R/Nu_S
4040	1.90
4041	2.3–2.4
4042	2.3–2.6
4043	2.5–3.5–3.1
4044	2.7–4.5–3.7
4045	2.8–5.5–4.2
4030	2.3–2.2
4031	2.7–3.4–3.0
4032	2.7–3.9–3.4
4033	3.0–5.0–4.6
4034	3.6–7.3–6.3
4035	3.6–9.6–7.4

mentation entropy generation number

$$N_S = \frac{\dot{S}_{gen,R}}{\dot{S}_{gen,S}} \tag{11}$$

Augmentation techniques with $N_S < 1$ are thermodynamically advantageous, since in addition to the enhanced heat transfer, they reduce the degree of irreversibility of the apparatus. The augmentation entropy generation number can be rewritten as [13,14]

$$N_S = \frac{N_T + \phi_o N_P}{1 + \phi_o}, \tag{12}$$

where [15]

$$N_T = \frac{(\dot{S}_{gen,\Delta T})_R}{(\dot{S}_{gen,\Delta T})_S} = \frac{Q_* \vartheta_{o,R} T_{o,S}}{N_* \vartheta_{o,S} T_{o,R}} \tag{13}$$

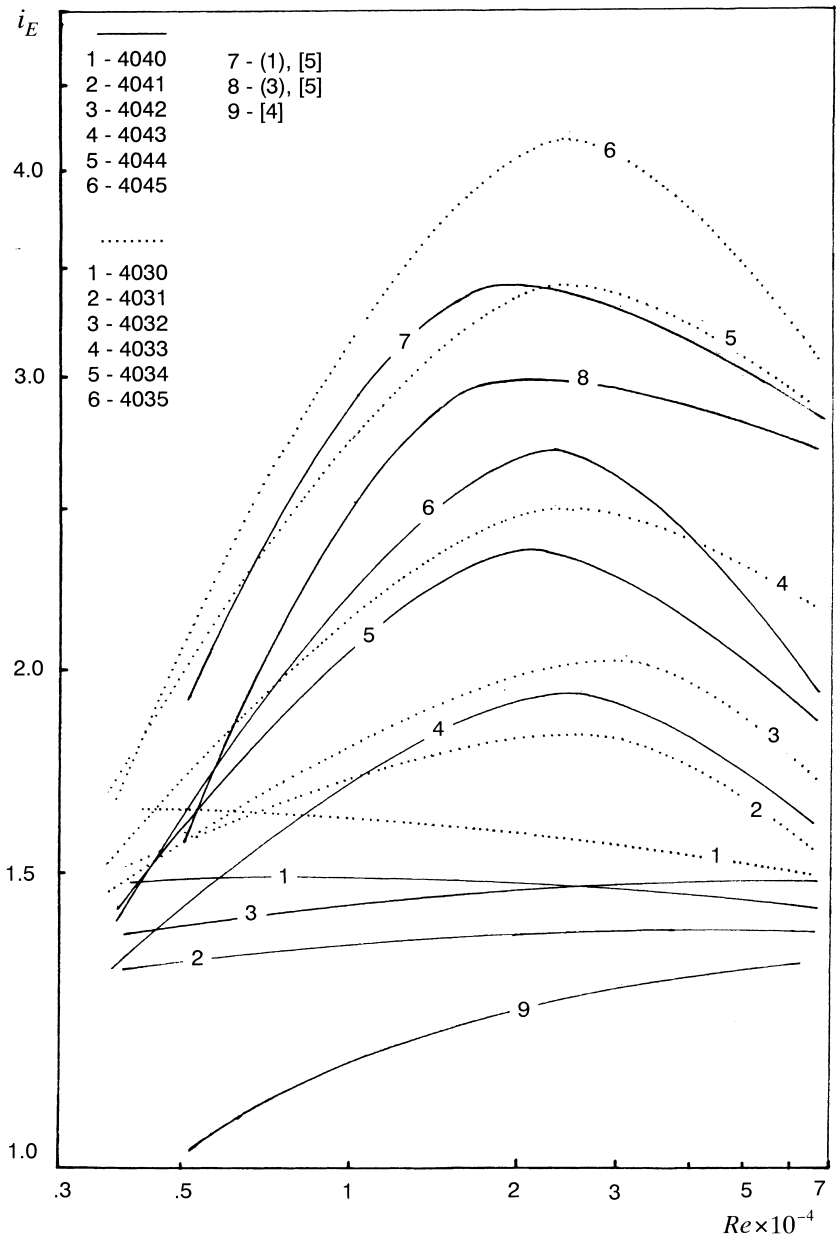

Fig. 5. Evaluation of heat transfer efficiency based on the constant energy dissipation.

$$\frac{T_{o,\mathrm{S}}}{T_{o,\mathrm{R}}} = \left[\frac{T_{i,\mathrm{S}}}{T_{o,\mathrm{S}}} + \frac{Q_*}{W_*}\left(1 - \frac{T_{i,\mathrm{S}}}{T_{o,\mathrm{S}}}\right)\right]^{-1}, \tag{14}$$

$$\frac{\vartheta_{o,\mathrm{R}}}{\vartheta_{o,\mathrm{S}}} = \exp\left[B\left(1 - \frac{St_\mathrm{R}}{St_\mathrm{S}}\frac{L_*}{D_*}\right)\right], \tag{15}$$

$$B = \frac{4St_\mathrm{S}}{D_\mathrm{S}} L_\mathrm{S}, \tag{16}$$

$$N_P = \frac{(\dot{S}_{\mathrm{gen},\Delta P})_\mathrm{R}}{(\dot{S}_{\mathrm{gen},\Delta P})_\mathrm{S}} = \frac{W_*^3 L_*}{N_*^3 D_*^5}\frac{T_{\mathrm{w,S}}}{T_{\mathrm{w,R}}}\frac{f_\mathrm{R}}{f_\mathrm{S}} = P_*\frac{T_{\mathrm{w,S}}}{T_{\mathrm{w,R}}} \tag{17}$$

When the standard heat transfer passage is known, the numerical value of the irreversibility distribution ratio, $\phi_\mathrm{o} = (\dot{S}_{\mathrm{gen},\Delta P}/\dot{S}_{\mathrm{gen},\Delta T})_\mathrm{S}$, describes the thermodynamic mode in which the passage is meant to operate [15]

$$\phi_\mathrm{o} = \frac{2f_\mathrm{S}L_\mathrm{S}}{D_\mathrm{S}}\left(\frac{u_\mathrm{m}^2}{c_p T_\mathrm{w}}\right)_S \frac{T_{\mathrm{i,S}}T_{\mathrm{o,S}}}{\vartheta_{\mathrm{o,S}}(T_\mathrm{o} - T_\mathrm{i})_\mathrm{S}}. \tag{18}$$

The solution to the PEC equations requires algebraic relations which:

1. Define correlations for $St(Nu)$ and f of the augmented surfaces as a function of Re.
2. Quantify performance objectives and design constraints. This means that the designer should define clearly his or her goal and then solve the equations, corresponding to the algebraic relations based on the first law of thermodynamics, to obtain the

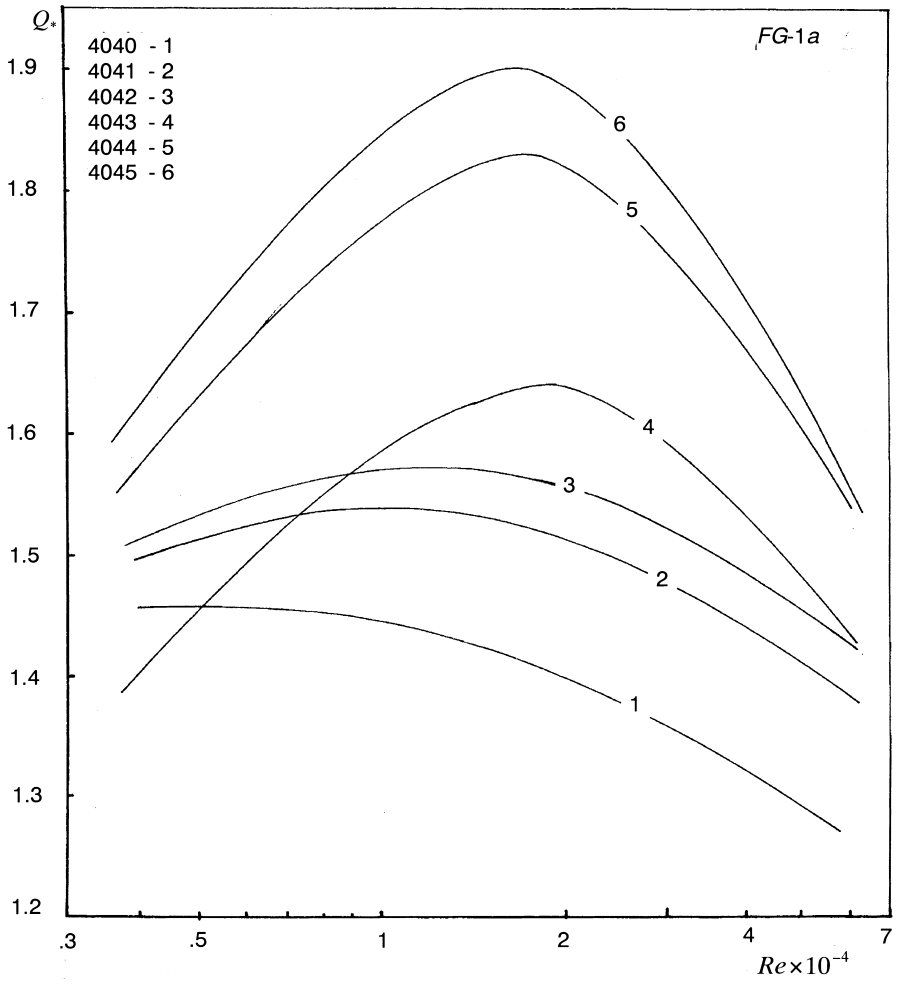

Fig. 6. Increased heat transfer rate vs. Reynolds number.

values of improved heat transfer rate, $Q_* = Q_R/Q_S$; reduced heat transfer area, $A_* = A_R/A_S$; or reduced pumping power, $P_* = P_R/P_S$ as a function of *Re*.

3. Calculate the irreversibility distribution ratio ϕ_o as a function of *Re* for the reference (smooth) passage.

The numerical values of ϕ_o (7.1×10^{-6}–0.16 in the range studied) show that the channel is dominated by heat transfer irreversibility. The effect of the thermal resistance external to the surface is also taken into consideration by including external heat transfer coefficient $h_{o,S}$. The analysis includes the possibility that the augmented exchanger may have an enhanced outer tube surface $E_o = h_{o,R}/h_{o,S}$. The fouling resistances on both sides of the tube wall are neglected.

The heat transfer efficiency of the tubes investigated has been evaluated for the following cases:

4.1. Fixed geometry criteria (FG)

These criteria involve a one-for-one replacement of smooth tubes by augmented ones of the same basic geometry, e.g. tube envelope diameter, tube length and

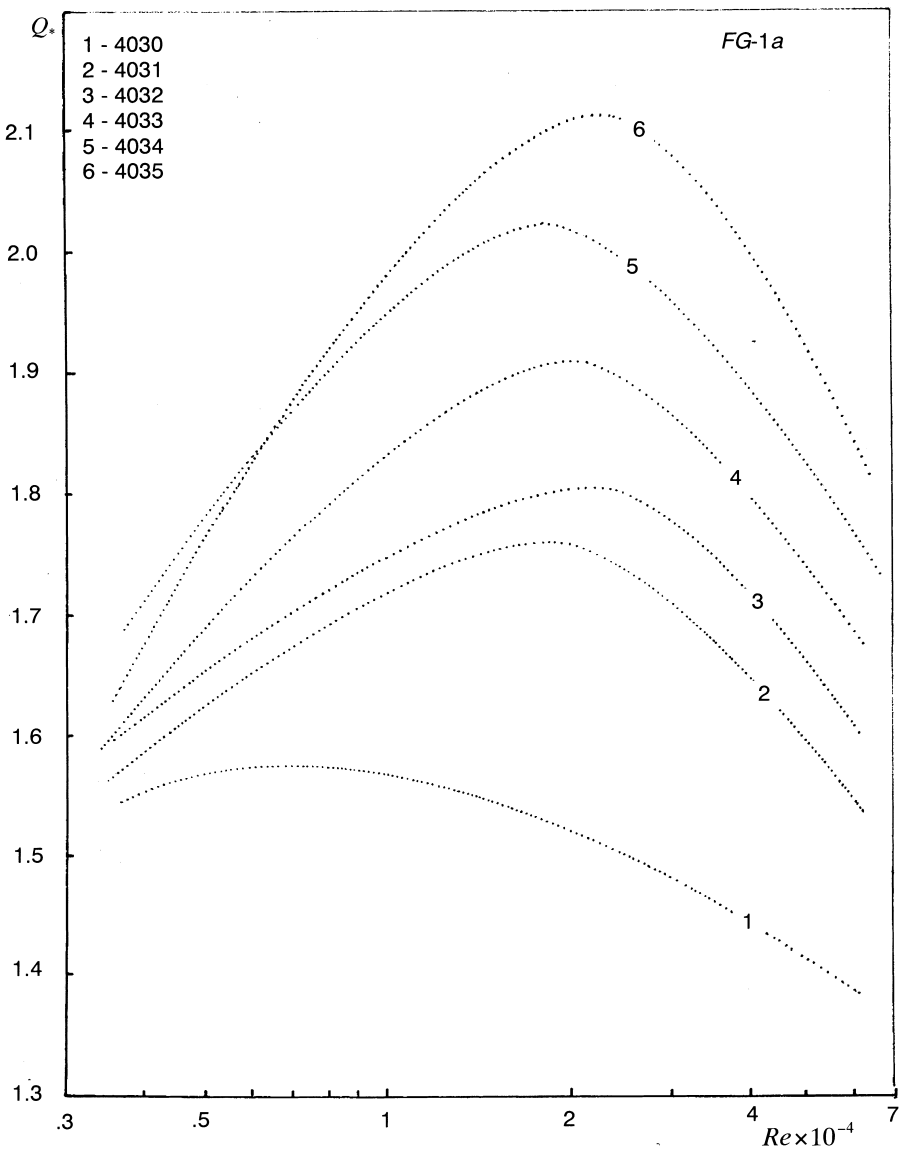

Fig. 7. Increased heat transfer rate vs. Reynolds number.

number of tubes for in-tube flow. The FG-1 cases [11,12] seek increased heat duty or overall conductance UA for the constant exchanger flow rate. The pumping power of the enhanced tube exchanger will increase due to the increased fluid friction characteristics of the augmented surface. For these cases the constraints $\Delta T_i^* = 1$, $W_* = 1$, $N_* = 1$ and $L_* = 1$ require $Re_S = D_* Re_R$ and $P_* > 1$.

When the objective is increased heat duty $Q_* > 1$, this corresponds to the case FG-1a [11,12]. In this case, the heat duty of the unit with spirally corrugated tubes combined with a twisted tape increases significantly; approaching the values of the order of 1.9 (for tube no. 4045), Fig. 6 and 2.1 (for tube no. 4035), Fig. 7, for the smallest relative pitch H/D_i, whereas the unit with spirally corrugated tubes alone attain the

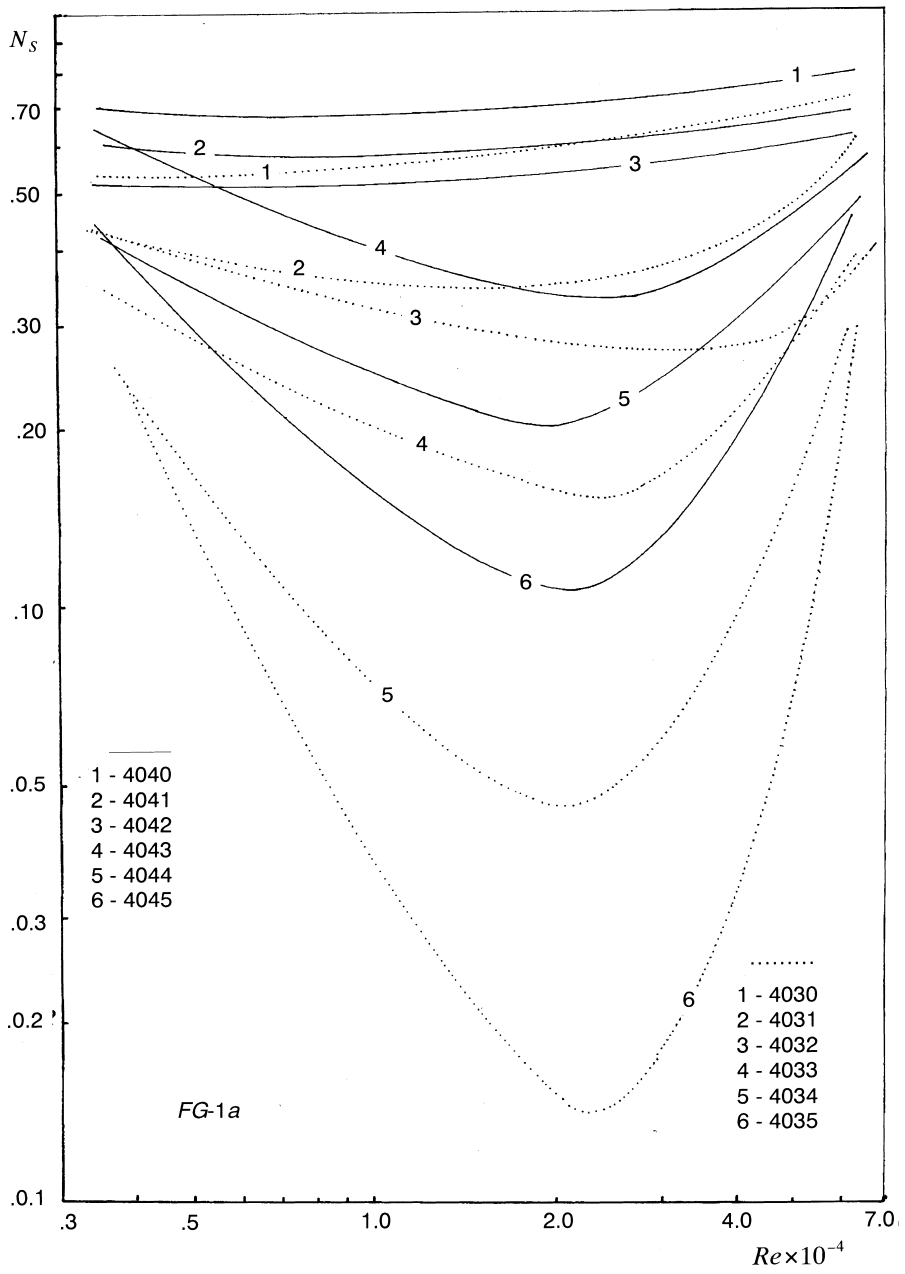

Fig. 8. Augmentation entropy generation number vs. Reynolds number.

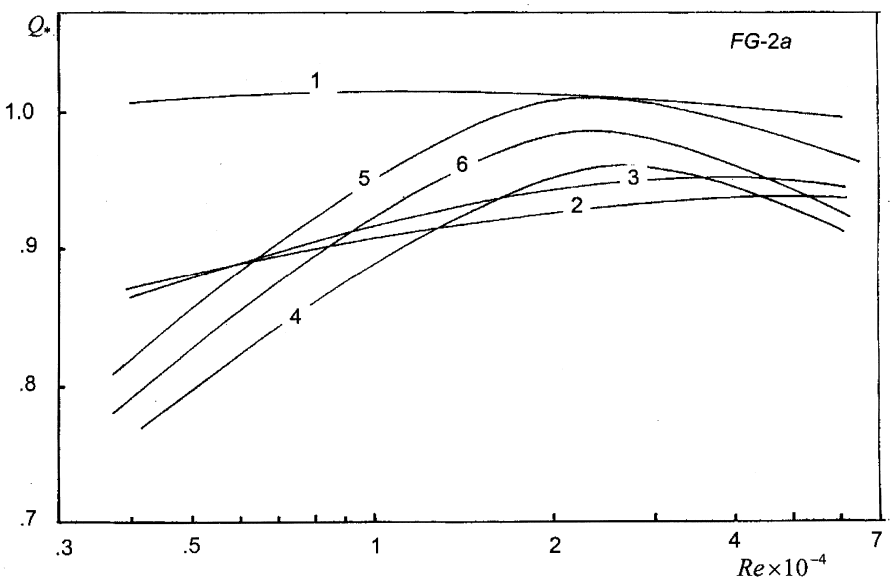

Fig. 9. Increased heat transfer rate vs. Reynolds number.

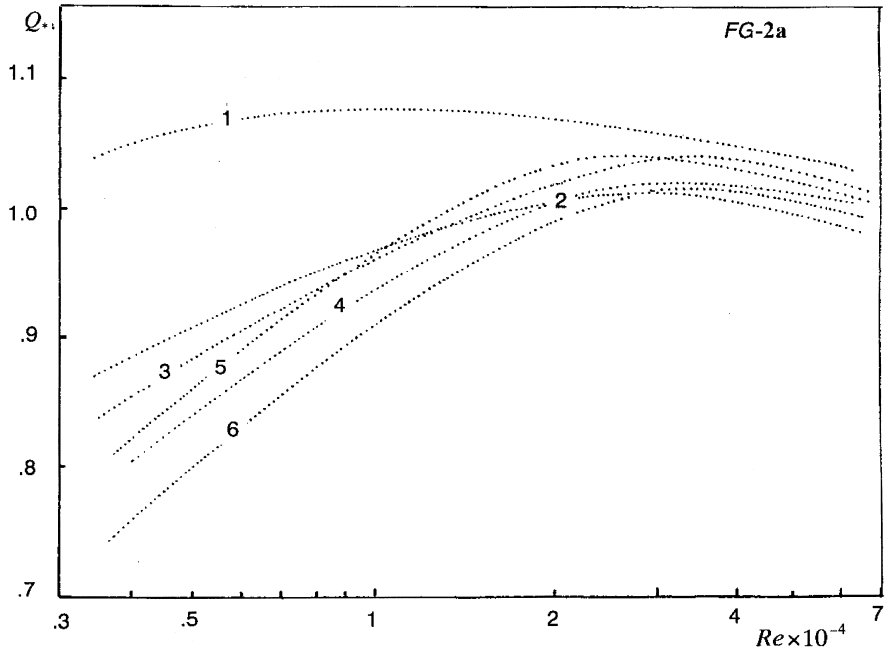

Fig. 10. Increased heat transfer rate vs. Reynolds number.

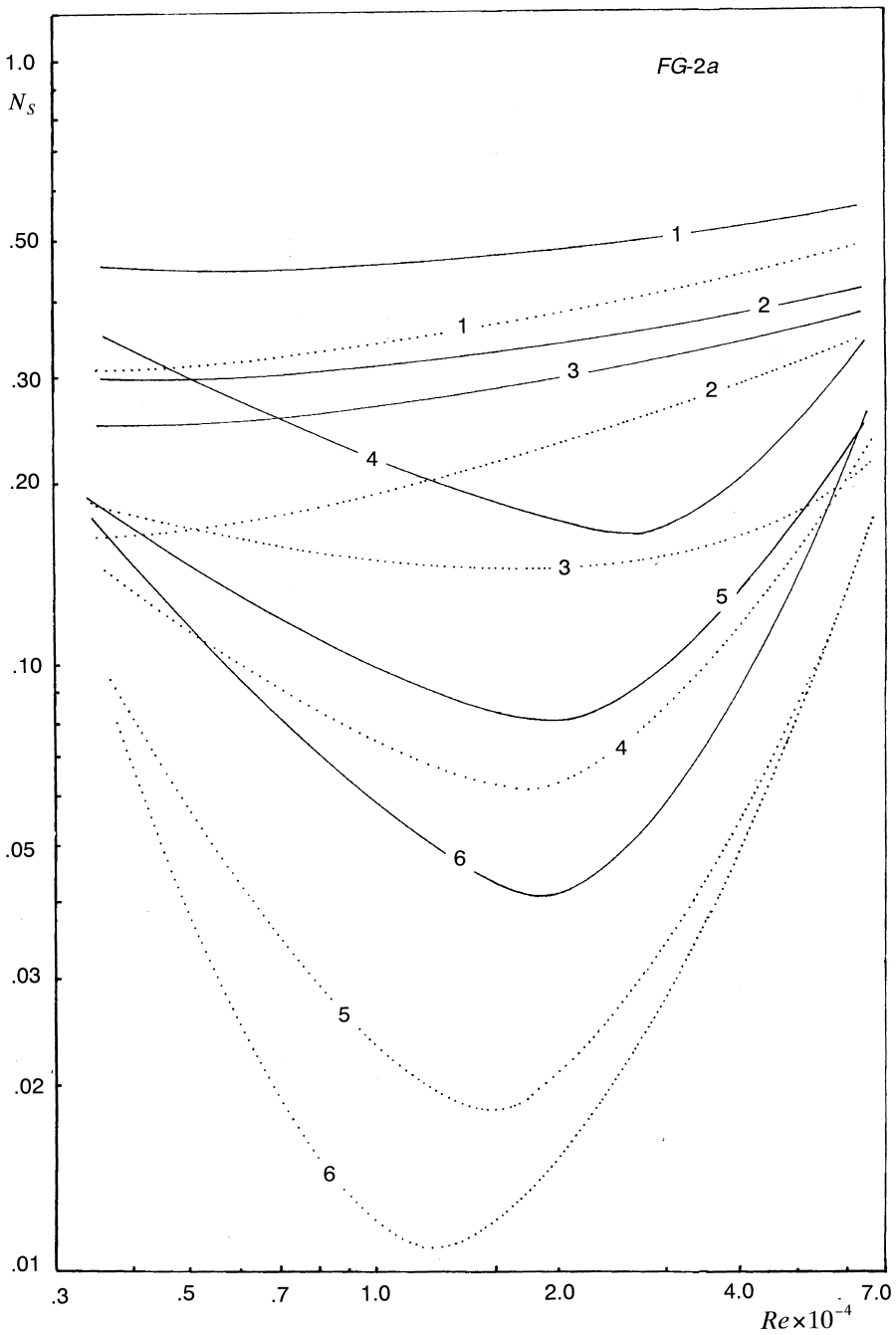

Fig. 11. Augmentation entropy generation number vs. Reynolds number.

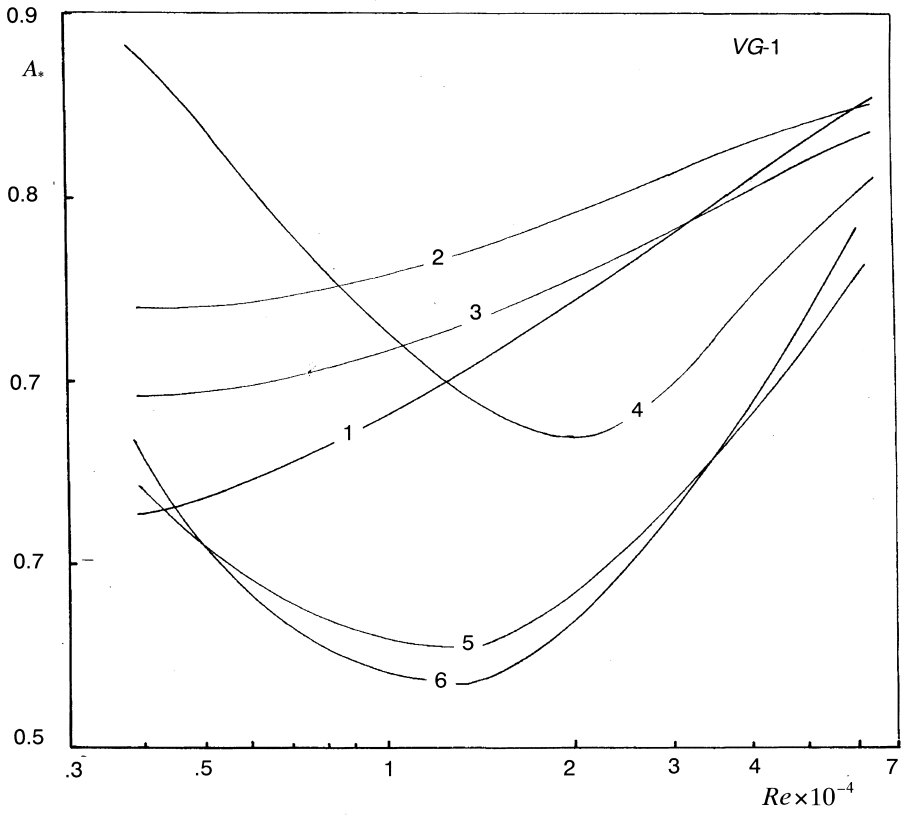

Fig. 12. Reduced surface area vs. Reynolds number.

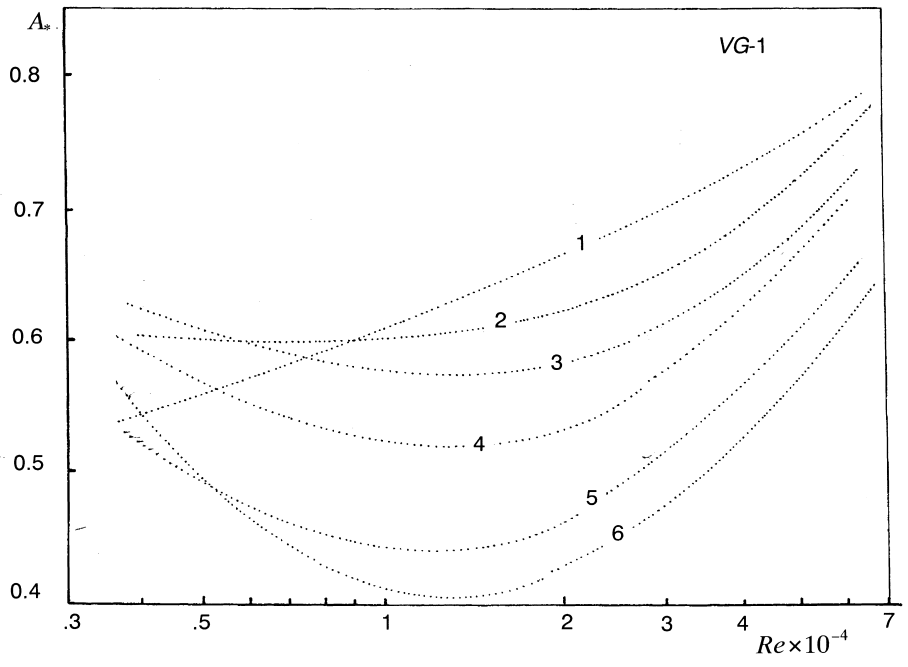

Fig. 13. Reduced surface area vs. Reynolds number.

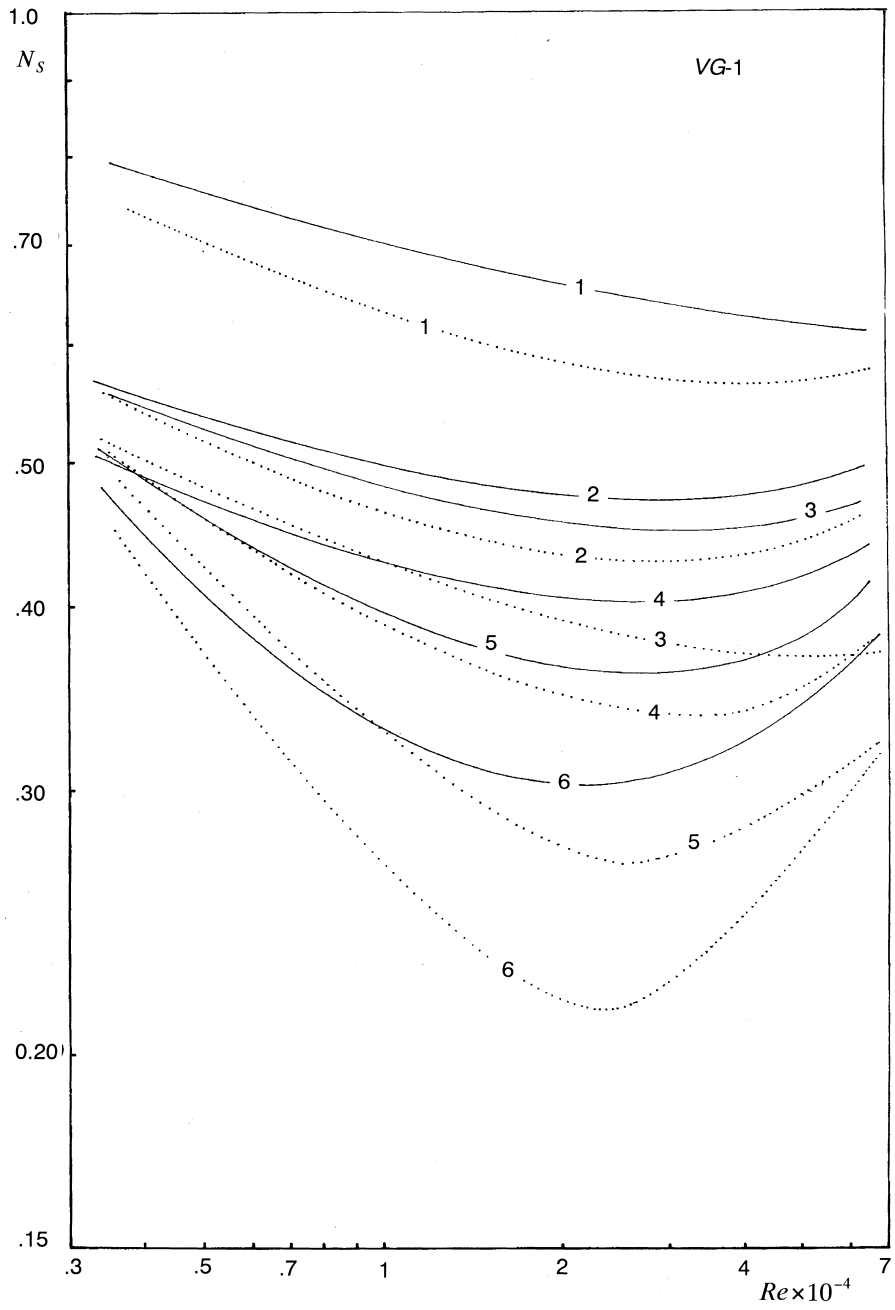

Fig. 14. Augmentation entropy generation number vs. Reynolds number.

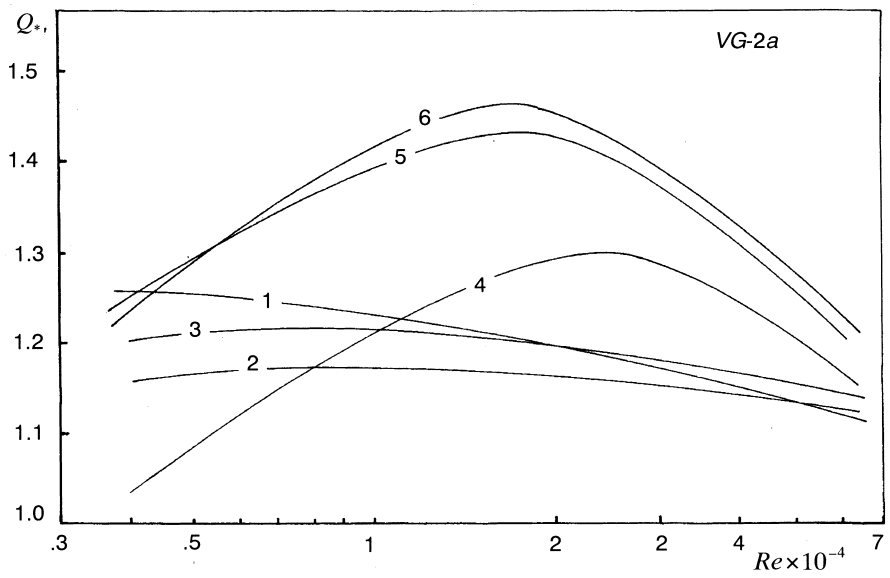

Fig. 15. Increased heat transfer rate vs. Reynolds number.

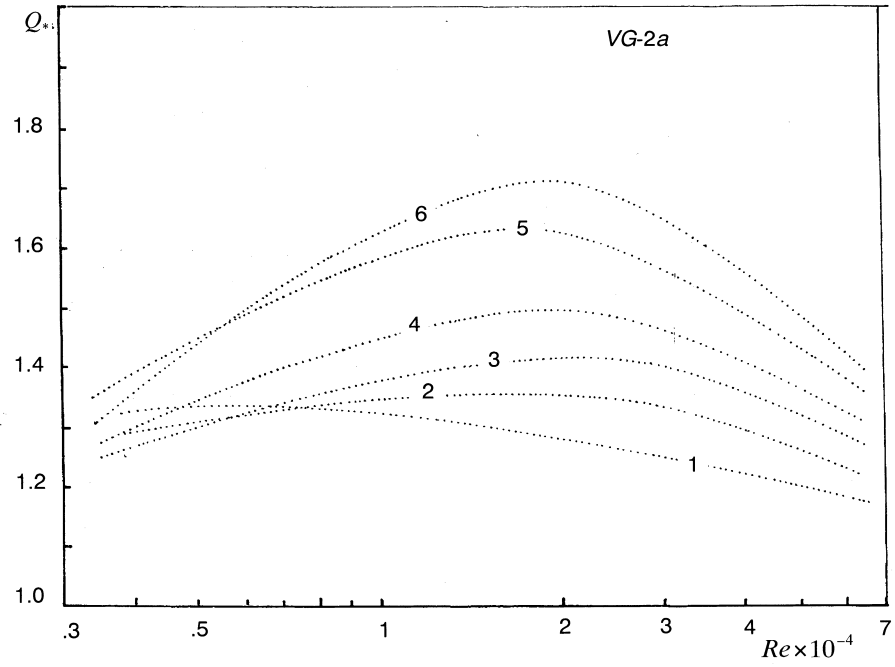

Fig. 16. Increased heat transfer rate vs. Reynolds number.

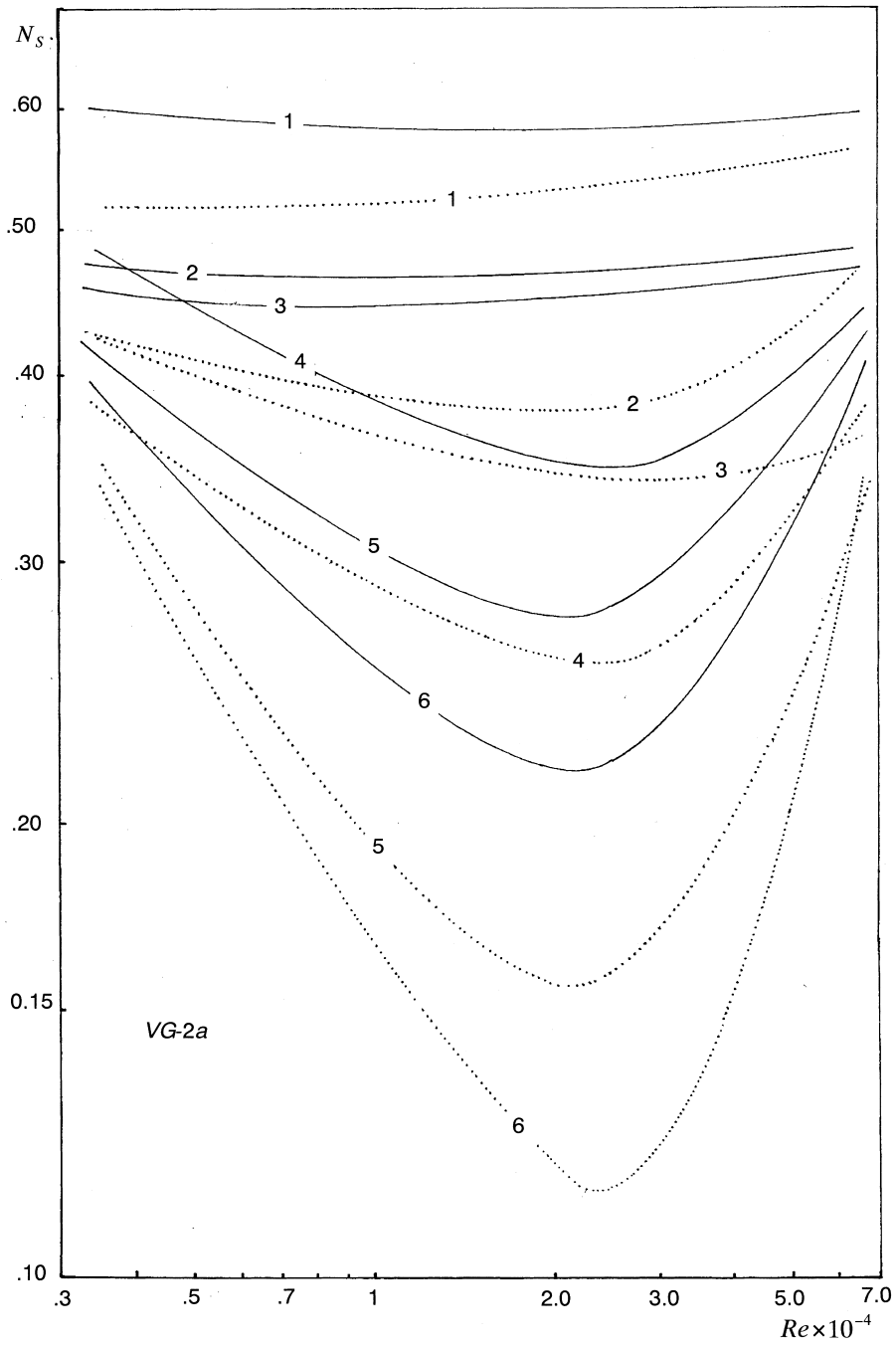

Fig. 17. Augmentation entropy generation number vs. Reynolds number.

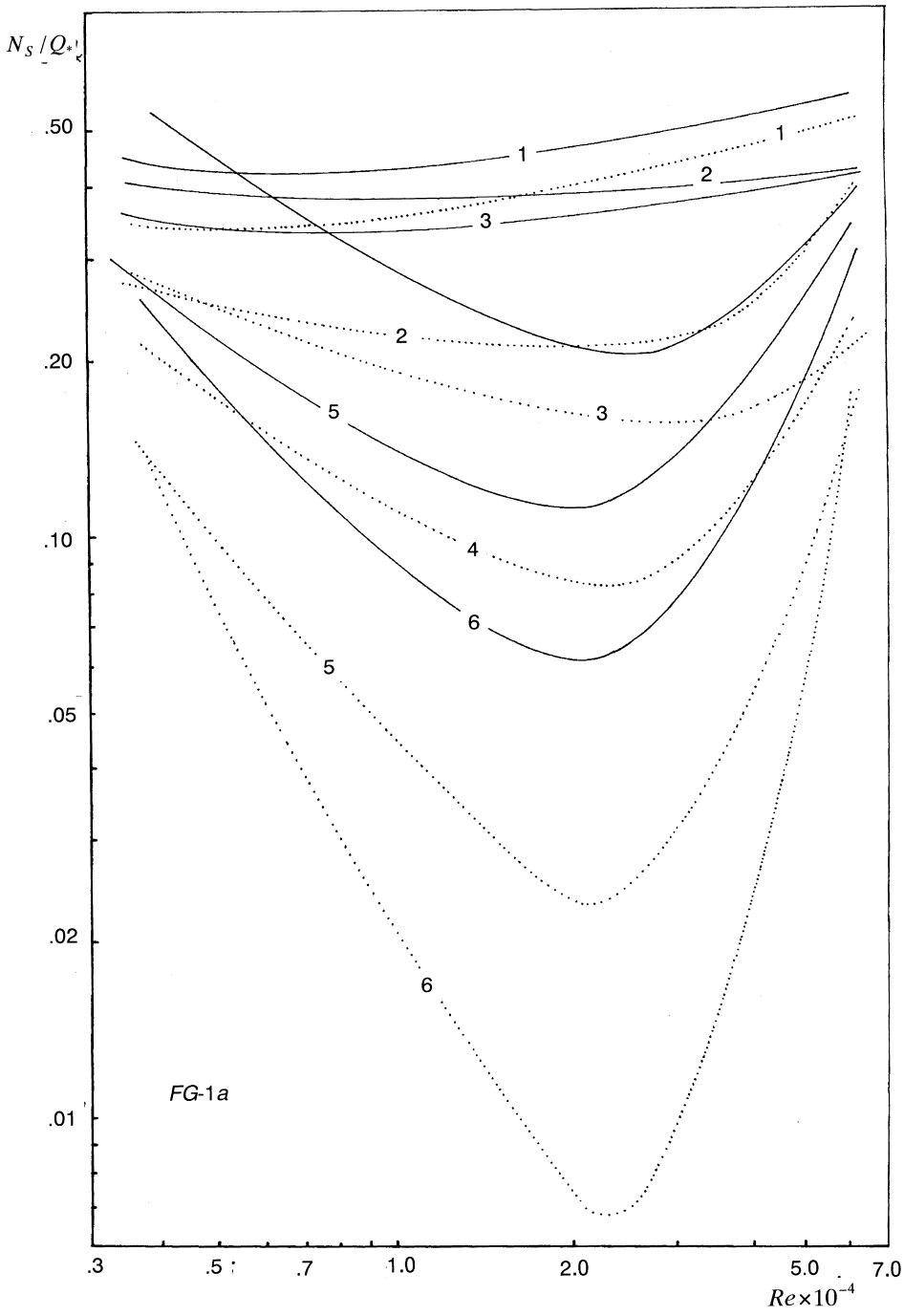

Fig. 18. The ratio N_S/Q_* vs. the Reynolds number.

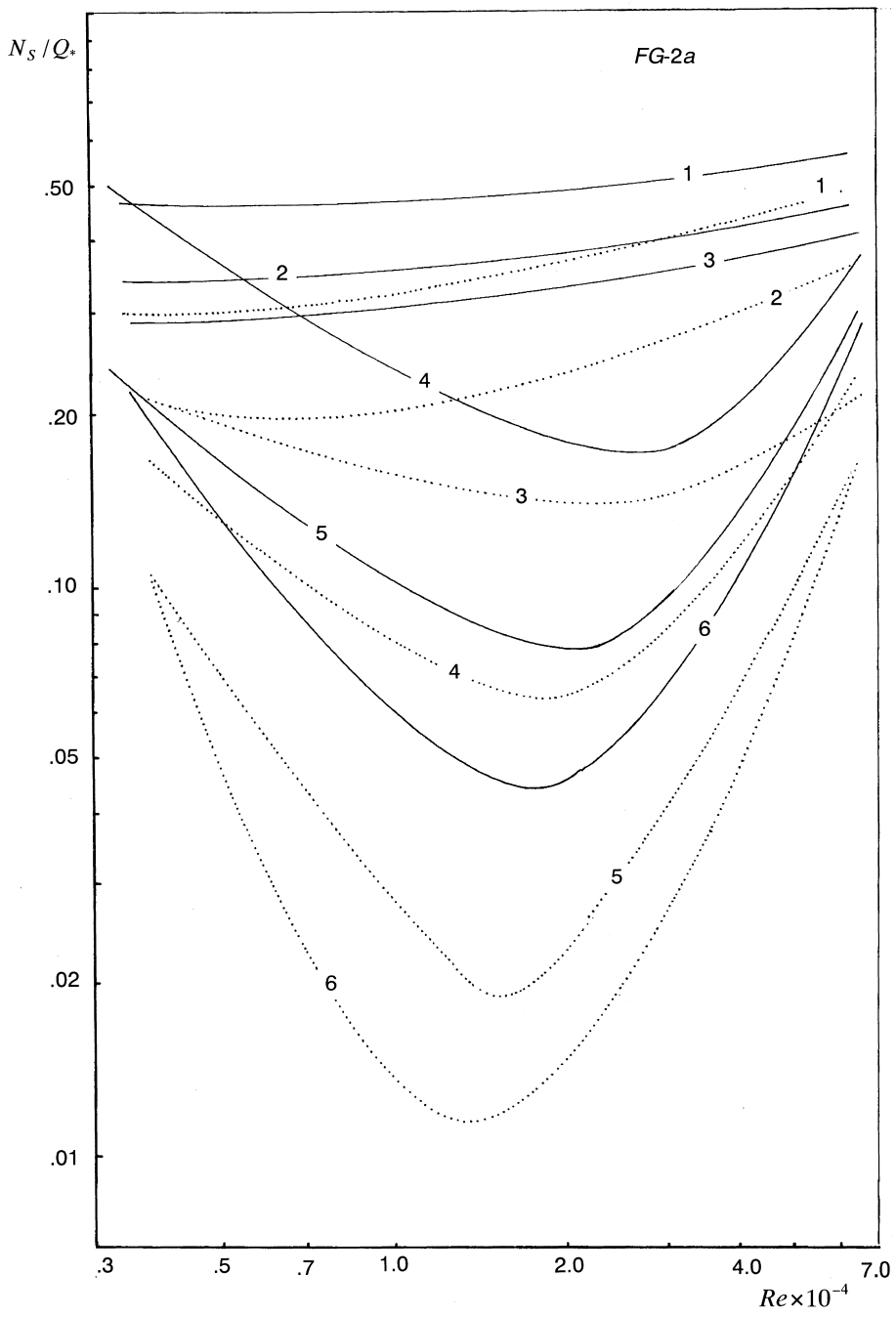

Fig. 19. The ratio N_S/Q_* vs. the Reynolds number.

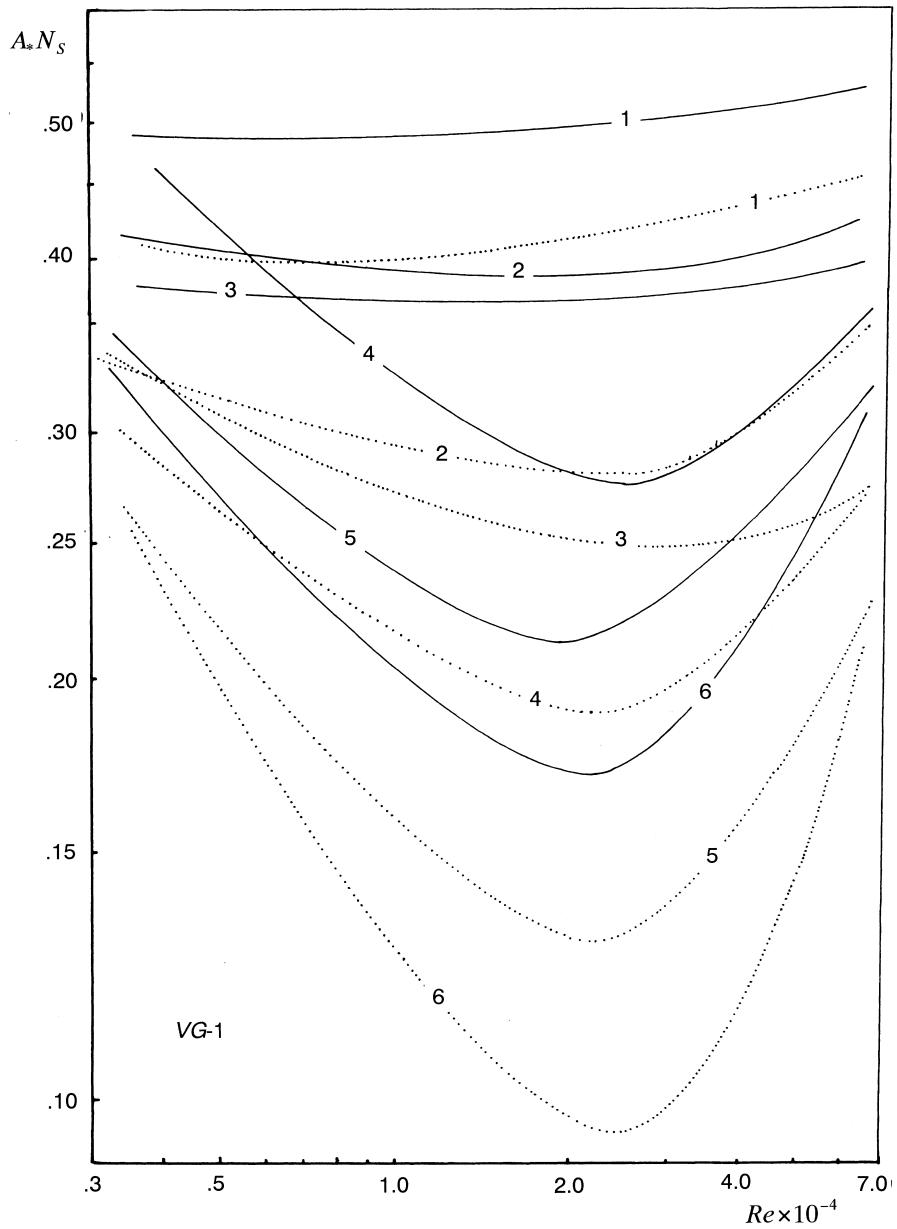

Fig. 20. The group A_*N_* vs. the Reynolds number.

values of $Q_* = 1.4$–1.5, Figs. 6 and 7. The augmentation entropy generation number N_S is [15]

$$N_S = \frac{1}{1+\phi_o}\left\{Q_* \exp\left[B\left(1-\frac{St_R}{St_S}D_*^{-0.8}\right)\right]\left[\frac{T_{i,S}}{T_{o,S}} + Q_*\left(1-\frac{T_{i,S}}{T_{o,S}}\right)\right]^{-1} + \phi_o \frac{f_R/f_S}{D_*^{4.75}}\right\} = f(Re_R). \quad (19)$$

As can be seen from Fig. 8 all the tubes reduce the entropy generation evaluated through the number N_S. The values of N_S for the corrugated tubes applied alone are 0.6–0.7. When the compound enhancement technique of this kind is applied, the values of N_S approach 0.10–0.02 for the smallest relative pitch H/D_i.

The FG-2 [11,12] criteria have the same objectives as FG-1, but require that the augmented tube unit should operate at the same pumping power as the reference smooth tube unit. The pumping power is remained as constant by reducing the tube-side velocity and thus the exchanger flow rate. The constraints are: $N_* = 1$, $L_* = 1$ and $P_* = 1$ requiring $W_* < 1$ and $Re_R < Re_S$. In the case FG-2a, the goal is to increase the heat transfer rate $Q_* > 1$. For this reason, the corrugated tubes alone have the values of $Q_* = 1.0$–1.05, Figs. 9 and 10, whereas for all the combinations of corrugated tubes and twisted tape inserts $Q_* < 1$. The augmentation

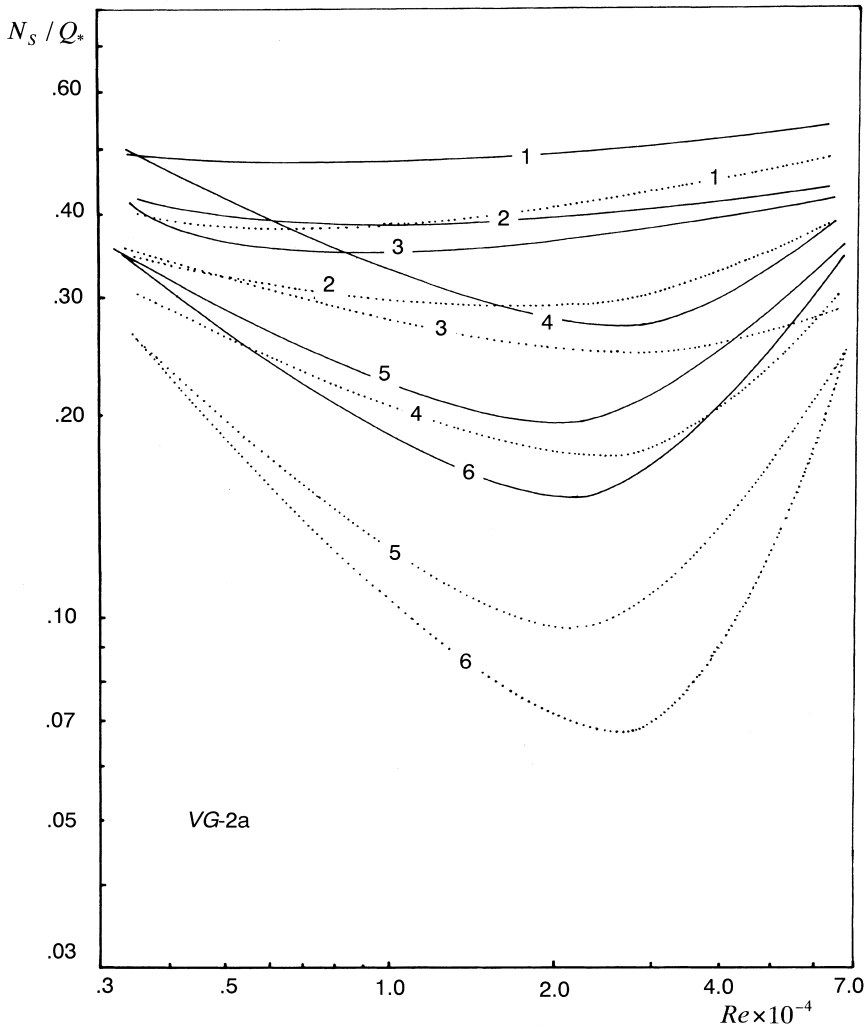

Fig. 21. The ratio N_S/Q_* vs. the Reynolds number.

entropy generation number N_S is [15]

$$N_S = \frac{1}{1+\phi_o}\left\{Q_* \exp\left[B\left(1-\frac{St_R}{St_S}D_*^{-1.145}\left(\frac{f_R}{f_S}\right)^{0.073}\right)\right]\left[\frac{T_{i,S}}{T_{o,S}}+Q_*\left(\frac{f_R}{f_S}\right)^{0.364}D_*^{-1.727}\left(1-\frac{T_{i,S}}{T_{o,S}}\right)\right]^{-1}+\phi_o\right\} = f(Re_R). \quad (20)$$

Despite of the fact that the goal imposed by the first law has not been achieved $Q_* < 1$ as can be seen from Fig. 11, the entropy generation number is substantially diminished. The value of the N_S reaches 0.45–0.35 for corrugated tube alone and attains 0.04–0.015 for the compound enhancement technique.

4.2. Variable geometry criteria (VG)

In most of the cases a heat exchanger is designed for a required thermal duty with a specified flow rate. Since the tube-side velocity must be reduced to accommodate the higher friction characteristics of the augmented surface, it is necessary to increase the flow area to maintain $W_* = 1$ and permit the exchanger flow frontal area to vary in order to meet the pumping power constraint: $N_* > 1$; $L_* < 1$; $Re_R < Re_S$. In the case of VG-1 [11,12] the objective is to reduce the surface area $A_* < 1$ with $W_* < 1$ for $Q_* = P_* = 1$.

In this case the reduction of heat transfer area is 30–40% when the corrugated tubes are used alone and 45–60% when they are combined with a twisted tape having the smallest relative pitch, Figs. 12 and 13. The entropy generation number is calculated from [15]

$$N_S = \frac{1}{1+\phi_o}\left\{\left(\frac{f_R}{f_S}A_*\right)^{-0.364}D_*^{2.091}\exp\left[B\left(1-\frac{St_R}{St_S}\left(\frac{f_R}{f_S}\right)^{-0.291}A_*^{0.709}D_*^{-0.127}\right)\right]+\phi_o\right\} = f(Re_R). \quad (21)$$

The reduction of the entropy generation is also significant, $N_S = 0.7$–0.6 for the corrugated tubes alone and $N_S = 0.3$–0.2 for the compound enhancement technique, Fig. 14.

The cases VG-2 [11,12] aim at increased thermal performance ($U_R A_R / U_S A_S$ or $Q_* > 1$) for $A_* = 1$ and $P_* = 1$. They are similar to the cases FG-2. When the objective is $Q_* > 1$, case VG-2a [11,12], an additional constraint is $\Delta T_i^* = 1$. The last case is considered to be VG-2a, where the objective is to increase the heat rate $Q_* > 1$ for $W_* = 1$ and $A_* = P_* = 1$. When the unit is furnished with corrugated tubes alone $Q_* = 1.15$–1.25, Figs. 15 and 16. When a combination with a twisted tape is used the values of Q_* reach 1.45–1.70. The values of N_S are calculated following [15]

$$N_S = \frac{1}{1+\phi_o}\left\{Q_*\left(\frac{f_R}{f_S}\right)^{-0.364}D_*^{2.091}\exp\left[B\left(1-\frac{St_R}{St_S}\left(\frac{f_R}{f_S}\right)^{-0.291}D_*^{-0.127}\right)\right]\left[\frac{T_{i,S}}{T_{o,S}}+Q_*\left(1-\frac{T_{i,S}}{T_{o,S}}\right)\right]^{-1}+\phi_o\right\} = f(Re_R), \quad (22)$$

and as can be seen from Fig. 17 the values are as follows: 0.60–0.55 for corrugated tubes alone and 0.25–0.15 for a compound enhancement technique.

The results discussed imply that the evaluation and comparison of the heat transfer augmentation techniques should be made on the basis of both first and second law analysis. Thus it is possible to determine the thermodynamic optimum in a heat exchanger by minimizing the augmentation entropy generation number compared with the relative increase of heat transfer rate $Q_* > 1$, or relative reduction of heat transfer area $A_* < 1$ or pumping power $P_* < 1$. Consequently, a ratio N_S/Q_* and a group $N_S A_* = f(Re_R)$ might be defined to connect the two objectives pursued by the first and second law analysis and as a basis for thermodynamic optimization.

Figs. 18–21 show $N_S/Q_* - Re_R$ for the cases FG-1a, 2a and VG-2a, and $N_S A_* - Re_R$ for the case VG-1. From all the cases considered the best performance has the tube 4035 being far superior to others. The benefit of making use of this tube is significant. Figs. 18–21 also show that most of the tubes to be considered have an optimum Reynolds number, corresponding to the minimum rate of entropy generation.

5. Conclusions

1. Heat transfer and friction characteristics of two three-start spirally corrugated tubes combined with five twisted tape inserts have been experimentally investigated. The isothermal friction coefficients for straight flow and swirl flow in the corrugated tubes increase when the relative pitch H/D_i decreases. The values for f_R/f_S varied from 2.4 to 17.9 in the range of Re studied. The water side heat transfer coefficients were particularly high when a corrugated tube was combined with a twisted tape. An unexpected behavior of the ratio $Nu_R/Nu_S = f(Re)$ was observed when the relative pitch began to diminish. For most of the tubes the ratio Nu_R/Nu_S approaches maximum at $Re \sim 2.5 \times 10^4$ and then gradually decreases.

The values for Nu_R/Nu_S varied from 1.9 to 9.6 in the range of Re studied.

2. Extended PEC has been used to assess the benefits of replacing the smooth tubes with multi-start spirally corrugated tubes combined with twisted tape inserts. An additional increase of the heat transfer rate or reduction of heat transfer area up to 30% and more than those of the corrugated tube can be achieved by an appropriate combination of corrugated tube with twisted tape. The reduction of the entropy generation is also significant. The results discussed imply that the evaluation and comparison of the heat transfer augmentation techniques should be made on the basis of both first and second law analysis. Thus, it is possible to determine the thermodynamic optimum in a heat exchanger by minimizing the augmentation entropy generation number compared with the relative increase of heat transfer rate $Q_* > 1$, or reduction of heat transfer area $A_* < 1$. Consequently, a ratio N_S/Q_* and a group $N_S A_* = f(Re_R)$ might be defined as a basis for a thermodynamic optimization.

References

[1] A.E. Bergles, The imperative to enhance heat transfer, in: Energy Conservation Through Heat Transfer Enhancement of Heat Exchangers, NATO Advanced Study Institute, Izmir, Turkey, 1998, pp. 547–563.

[2] A.E. Bergles, M.K. Jensen, B. Shome, Bibliography on enhancement of convective heat and mass transfer, RPI Heat Transfer Laboratory Report HTL-23, New York, 1995.

[3] C.A. Balaras, A review of augmentation techniques for heat transfer surfaces in single-phase heat exchangers, Energy 15 (10) (1990) 899–906.

[4] A.E. Bergles, R.A. Lee, B.B. Mikic, Heat transfer in rough tubes with tape-generated swirl flow, transaction of the ASME, J. Heat Transfer 91 (1969) 443–445.

[5] H. Usui, Y. Sano, K. Iwashita, A. Isozaki, Enhancement of heat transfer by a combination of internally grooved rough tube and a twisted tape, Int. Chem. Eng. 26 (1) (1986) 97–104.

[6] V.D. Zimparov, N.L. Vulchanov, L.B. Delov, Heat transfer and friction characteristics of spirally corrugated tubes for power plant condensers — 1. Experimental investigation and performance evaluation, Int. J. Heat Mass Transfer 34 (9) (1991) 2187–2197.

[7] V. Gnielinski, New equations for heat and mass transfer in turbulent pipe and channel flow, Int. Chem. Eng. 16 (1976) 359–368.

[8] R.L. Webb, E.R.G. Eckert, Application of rough surfaces to heat exchanger design, Int. J. Heat Mass Transfer 21 (1972) 1647–1658.

[9] A.E. Bergles, A.R. Blumenkrantz, J. Taborek, Performance evaluation criteria for enhanced heat transfer surfaces, Fifth International Heat Transfer Conference, Tokyo, 5, FC 6.3, 1974, pp. 239–243.

[10] A.E. Bergles, R.L. Bunn, G.H. Junkhan, Extended performance evaluation criteria for enhanced heat transfer surfaces, Lett. Heat Mass Transfer 1 (1974) 113–120.

[11] R.L. Webb, Performance evaluation criteria for use of enhanced heat transfer surfaces in heat exchanger design, Int. J. Heat Mass Transfer 24 (1981) 715–726.

[12] R.L. Webb, A.E. Bergles, Performance evaluation criteria for selection of heat transfer surface geometries used in low Reynolds number heat exchangers, in: NATO Advanced Study Institute, 1981, Ankara, Turkey, Low Reynolds Number Heat Exchangers, Hemisphere, Washington, DC, 1983, pp. 735–752.

[13] A. Bejan, Entropy Generation Through Heat and Fluid Flow, Wiley, New York, 1982.

[14] A. Bejan, Entropy Generation Minimization, CRC Press, Boca Raton, FL, 1996.

[15] V.D. Zimparov, Extended performance evaluation criteria for heat transfer surfaces: heat transfer through ducts with constant wall temperature, Int. J. Heat Mass Transfer 43 (17) (2000) 3137–3155.

[16] R.M. Nelson, A.E. Bergles, Performance evaluation criteria for tube side heat transfer enhancement of a flooded evaporator water chiller, ASHRAE Trans. 92 (1) (1986) 739–755.

[17] W.J. Marner, A.E. Bergles, J.M. Chenoweth, On the presentation of performance data for enhanced tubes used in shell-and-tube heat exchangers, transaction of the ASME, J. Heat Transfer 105 (1983) 358–365.